Research Paper

Integrated, Molecularly Imprinted Polymeric Membranes for the Concentration of BPA in a Capacitive Deionization Process

Joanna Wolska *, Anna Siekierka *, Katarzyna Smolińska-Kempisty *

Wroclaw University of Science and Technology, Department of Process Engineering and Technology of Polymer and Carbon Materials, Wybrzeże Wyspiańskiego 27, 50-370 Wrocław, Poland

Highlights

- Paths of synthesis of the integrated heterogeneous membrane with MIPs
- New potential application of the molecularly imprinted polymers
- Quickly method for monitoring and concentration of BPA via CDI process

Graphical abstract

Abstract

Molecularly imprinted polymers (MIP) toward bisphenol A (BPA) in the shape of microspheres with an average sphere size of 40 μm were obtained by a two-step process of membrane emulsification and then suspension polymerization. The prepared materials were used for the removal of BPA from the real and model aqueous solutions. The synthesized microspheres were then integrated into thin solid membranes made of poly(vinyl chloride) (PVC). The imprinted merged membranes were used in the capacitive deionization process to concentrate the amount of bisphenol A in aqueous solutions. The 30-minute process allowed a bisphenol A concentration of 63.7%. Three sorption/desorption cycles were performed. The total sorption capacity of BPA reached more than 80 mg/g. In all of these cases, a concentration of bisphenol A was achieved of more than 60%. The tests were also repeated after three months. The efficiency of the membranes decreased to ~ 18% of the concentration in one batch.

1. Introduction

The intensive development of technology also involves the development of the membrane sector. In 1950, the world market for membranes and membrane technology was just US $ 5 Million [1]. In 2020, it was already US $ 19.3 Billion. Despite the crisis caused by Covid-19 and the correction of the intensity of the increase in demand for membrane technologies, it is estimated that this market in 2026 will reach the value of US $ 30.9 Billion [2]. Such high values best illustrate the demand for membranes and related technologies. The possibilities for using membranes are highly extensive [3]. An example of using this kind of materials in advanced chemical processes can be prepared by us a new, integrated membrane capable of concentrating the amount of hazardous bisphenol A (BPA) in an aqueous solution in the electrochemical process.

Hazardous substances, such as compounds from the group of endocrine disruptors, can be present in water in trace amounts [4]. Small micropollutants are often beyond the detection threshold of commercially available measurement methods. This gives the illusion that the analyzed water sample is not contaminated. Methods used to isolate trace chemicals from a sample, such as solid phase extraction, liquid-liquid extraction, accelerated solvent extraction, and membrane extraction, are frequently used [5-8]. However, they need to work better at thickening the selected compound. Mainly due to their low selectivity and blocking of the bed when filtering larger amounts of the sample [9]. In addition, it is necessary to use organic solvents in the analyte elution step [6-9]. For this reason, we decided to develop an integrated
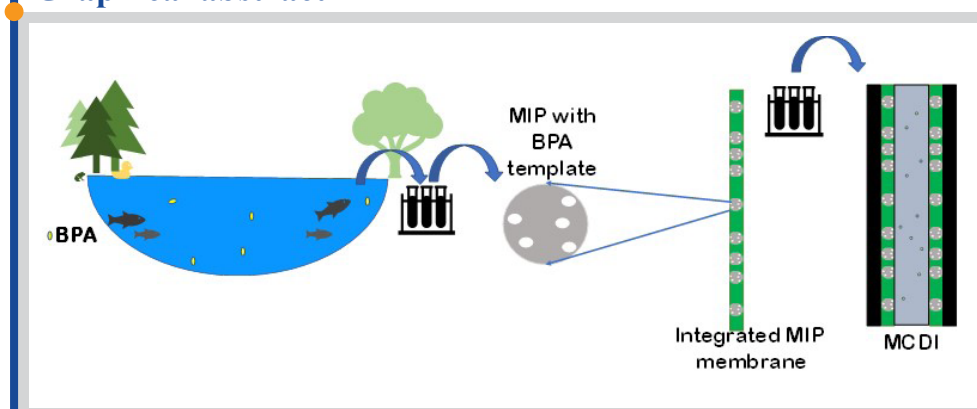
* Corresponding authors: joanna.wolska@pwr.edu.pl (J. Wolska), anna.siekierka@pwr.edu.pl (A. Siekierka); katarzyna.smolinska@pwr.edu.pl (K. Smolinska)

membrane capable of participating in the chemical concentration process. These membranes, in the form of a film with the molecularly imprinted polymer (MIP), allow for effective and rapid concentration of a selected sample component because of the high affinity of the molecular imprints to the analyte. The process is carried out in an aqueous solution, which allows the complete elimination of organic solvents and fits perfectly into the trends of "green chemistry".

The selective concentration of molecules is an effect of the presence of MIPs in the membrane. The phenomenon of affinity and selectivity in the template is possible due to the specific synthesis of these polymers. In the first step of MIP synthesis, a pre-polymerization complex is formed between the functional monomers and the template molecule. Next, the polymeric network is formed around the template in the effect of polymerization and crosslinking of the polymer chains. After the end of the synthesis, the template is removed, while the template-specific imprints remain in the polymer structure [10-15]. Therefore, MIPs have a wide range of applications [16,17]. They can be successfully used as a sensory material [18] in medicine applications [10,16,19,20] or as electrochemical sensors [18,21,22]. The number of publications that describe MIPs as sensory material in electrochemical applications is systematically increasing [18,23,24]. However, to the best of our knowledge, no MIPs have been used in the capacitive deionization process.

Electrochemical techniques are highly beneficial in water treatment [25]. One of the most widely used methods is membrane capacitive deionization – MCDI [26]. This is one of the Capacitive Deionization (CDI) method modifications. This process is based on the phenomenon of electrosorption of ionized matter. It is used primarily to remove dissolved particles from aqueous solutions [27,28], for seawater desalination [29], wastewater remediation [30], and softening of drinking water [31]. The primary MCDI cell comprises two parallel electrodes separated by a polymer separator that allows the liquid to flow between the electrodes. On the surface of carbon electrodes, membranes, usually ion exchange membranes, are placed [32]. The purpose of membranes is to selectively support the sorption/desorption process [26-28]. In the presented work, this technique was adapted to the selective concentrating of BPA (Fig. 1).
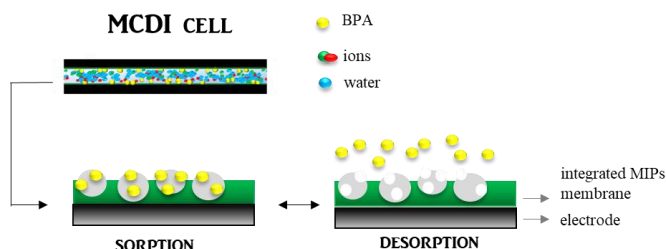

Fig. 1. Scheme of MCDI cell with integrated MIPs membrane.

2. Materials and Methods

2.1 Materials

Poly(vinyl chloride) (PVC) powder (Ongrovil® S-5167) in suspension polymer form, with medium molecular weight and with a K value (an indicator of molecular weight) of 66-68 supplied by BorsodChem, was used for the preparation of PVC films. Ethylenediamine (EDA) and bisphenol A (BPA) were acquired from Sigma-Aldrich Co. Tetrahydrofuran (THF), p-nitrophenol (NP), ethanol, and cyclohexanone (CH) were purchased from Avantor Performance Materials Ltd. (former POCh). The activated carbon (AC) YP-50F was prepared from coconuts supplied by Kuraray Chem Co., Japan. All reagents were used as received.

2.2. Preparation of microspheres

The synthesis of imprinted polymer (MIP) and non-imprinted polymer (NIP) in the shape of microspheres was described in our previous paper [13]. For their preparation, the two-step method was used, in which the membrane emulsification process was used in the first stage and then in the second stage the suspension polymerization. As functional monomers during polymers synthesis, N-isopropyl acrylamide and methyl methacrylate were used; furthermore, ethylene glycol dimethacrylate was used as a cross-linking agent. This study used MIP from the mixture with 5 wt.% of templates (BPA) (see Ref. 13).

2.3 Sorption from the real samples

To study the efficiency of BPA removal from real samples by MIP and NIP, approximately 0.1 g of dry polymer particles and 50 mL of 0.5 mmol/L BPA solution in tap water were mixed for 24 h at room temperature. After reaching equilibrium, the samples were filtrated and the supernatant was analyzed for the concentration of BPA that remained in the solution using a Jasco V–630 model spectrophotometer (λ_{max} = 276 nm). The sorption capacity, q_{BPA} (mmol/g), defined as the amount of BPA adsorbed at equilibrium, was then calculated from Equation (1).

$$q_{BPA} = \frac{(C_0 - C_e).V}{m} \tag{1}$$

where, C_o and C_e (mmol/L) are the initial concentration of BPA and its concentration at equilibrium, respectively, V (L) is the volume of solution, and m (g) is the mass of the dry polymer used [33].

Furthermore, the distribution coefficient (K_{BPA}) was calculated as a ratio of the amount of BPA adsorbed on 1 g of polymer and the amount of bisphenol A in equilibrium in 1 mL of solution (Equation (2)) [34]:

$$K_{BPA} = \frac{q_{BPA} \cdot \rho}{C_e} \tag{2}$$

where ρ (g/L) is the density of the BPA solution.

2.4. Competitive binding

A competitive sorption experiment was performed for two materials, MIP and NIP. About 0.1 g of dry polymer and 50 mL of the solution in the presence of bisphenol A and p-nitrophenol (NP). The initial concentration of each substance was 0.1 mmol/L. The mixtures were stirred for 24 hours at room temperature. After that time, the resins were filtrated and the solution was studied to determine the concentration of analytes using a Jasco V–630 model spectrophotometer. The detection was carried out at 230 nm for BPA and 318 nm for NF. After that, the distribution coefficient was calculated using Equation (2) [35].

Furthermore, the imprinting factor (IF) was calculated from Equation (3) [35, 36]:

$$IF = \frac{K_i^{MIP}}{K_i^{NIP}} \tag{3}$$

where $K_{i(j)}$ is the distribution coefficient (i, j = (BPA, NP)) of a substance on an imprinted polymer (K^{MIP}) and a non-imprinted polymer (K^{NIP}).

To obtain the specific selectivity factor (S), the ratio of IFs for two different substances (IF_i, IF_j) was calculated using Equation (4):

$$S = \frac{IF_i}{IF_j} \tag{4}$$

2.5 Preparation of membranes with microspheres

Thin polymer films with a thickness of 39.7 ± 4.8 μm were obtained by pouring them out of the 10 wt.% solutions of poly(vinyl chloride) in tetrahydrofuran using a casting knife. The films were allowed to evaporate in the air for 24 hours. In the next step, a suspension of molecularly imprinted polymers was prepared (0.3 g of MIPs were suspended in 10 mL of THF). Then it was applied to previously scheduled PVC films utilizing dropping. In this way, membranes containing molecularly imprinted polymers were obtained. The thickness of the material after modification was 92.5 ± 2.9 μm. The amount of MIPs incorporated into the films was 7.7 mg/cm², expressed in g MIP/cm².

The films thus obtained were then modified in 50 vol.%. ethylenediamine in ethyl alcohol at room temperature. The films were placed in the prepared EDA solution for 5 days. After this time, the membrane was washed successively with portions of ethanol, then 50:50 vol. ethanol and water, and finally with water to remove unreacted EDA.

The thickness of the membranes was measured with a micrometer screw. The amount of MIP expressed in mg/cm² was determined using the weight method.

2.6 Electrode preparation

The activated carbon YP-50F prepared from coconuts delivered by Kuraray Chem Co., Japan, was used as an active material for electrode building. First, the cathode and anode were prepared by mixing 90 wt.% of AC and 10

wt.% of poly(vinyl chloride) (PVC) solution in cyclohexanone (CH) (3.5% of PVC in CH), according to [37,38]. The AC paste in PVC/CH was then homogenized for 30 min at 40°C in an ultrasonic reactor (CNC-Ultrasonic, PS 30A). Finally, the slurry was cast on the current graphite collector, and electrodes with ~ 80 µm thickness by casting knife were formed. Next, the CH was removed by evaporation at 60°C for 24 h, and the electrodes were immersed in demineralized water and rinsed before application.

2.7 MCDI configuration and calculations

An electrodialyzer (FT-ED-100-4, FumaTech,) was employed as an MCDI cell assembly to study BPA removal and concentration. The MCDI stack comprised two parallel electrodes divided by a polymeric space channel with 200 µm thickness. The discovered foils covered both electrodes with inserted MIPs. The total thickness of the comminated electrodes was 120 µm.

The electrodialyzer was biased by a multi-range programmable DC Power Supply Korad KD3005D. The tests were carried out in constant current (CC) electrical mode. The concentration of BPA was monitored using the GBC Cintra 303 UV-VIS spectrophotometer at a wavelength of 276 nm.

Fundamental factors for the capacitive deionization process, such as the substance (BPA) adsorption capacity (SAC) and the BPA adsorption rate (ASAR), were evaluated. First, the SAC determined the sorbed BPA per gram of active material, which was considered the MIP (0.007 g/cm^2). Then, when the amount of adsorbed BPA was normalized to the processing time, it calculated the average bisphenol A adsorption/desorption rate. Then, the following metrics were energy normalized adsorption of BPA (ENAS) in gram units per Joule of energy. The next factor describing CDI was electrical work in Wh per gram of adsorbed bisphenol A. It was defined as the ratio of charge flow by the system during the adsorption step and the electrical potential between the electrodes in the mass of adsorbed BPA [39].

2.8 Scanning Electron Microscopy

Scanning electron microscopy (SEM) analysis of the MIP/NIP microspheres was performed using the JSM 5800LV microscope with an acceleration potential of 15 kV. To obtain a conductive surface, the MIPs spheres were coated with gold.

2.9 Optical microscope analysis

The surface of the membrane was analyzed using a TECHREBAL stereoscopic optical microscope. WF 20X/10 eyepiece was used. The camera with the following parameters was used: 16 million pixels and a matrix size: of 1/2.3"

3. Results and Discussions

3.1. Preparation of heterogenous MIPs wrapped membranes

Our previous paper characterized the preparation of MIP microspheres in a detailed way [13]. The microspheres were obtained in a two-step method, where the first step was to perform the membrane emulsification process in a commercial MICROPORE apparatus. SEM pictures of the imprinted polymers used to prepare the integrated membrane are shown in Fig. 2. Both imprinted (MIP – Fig. 2A) and non-imprinted (NIP – Fig. 2B) polymers were characterized by almost the exact shape of the spheres. In the micrographs, the developed porous structure of the obtained spheres can also be observed. The synthesized microspheres were used to prepare integrated materials which were then used in the electro-membrane process to concentrate one of the endocrine disruptors - BPA. Fig. 3 shows an optical microscope photo of the integrated membrane. It shows clusters of spherical MIPs. In some places, the spheres connect to form a single structure. This is the result of their very close positioning next to each other. In addition, these clusters look like a limit line surrounded by them; this is probably the effect of digestion formed in the poly(vinyl chloride) foil as a result of dissolving its surface at the integration stage with MIP spheres.

The MIP spheres do not completely cover the surface of the PVC film, so the spaces between them could have successfully reacted with EDA, increasing the effectiveness of the membrane in the MCDI process.
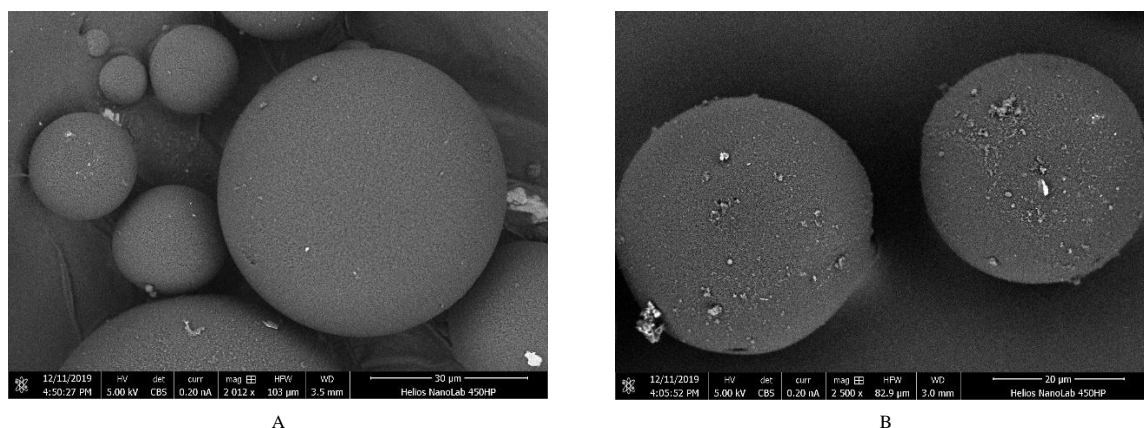

Fig. 2. Scanning electron microscopy (SEM) pictures of (A) – NIP, (B) – MIP, magnification × 5000
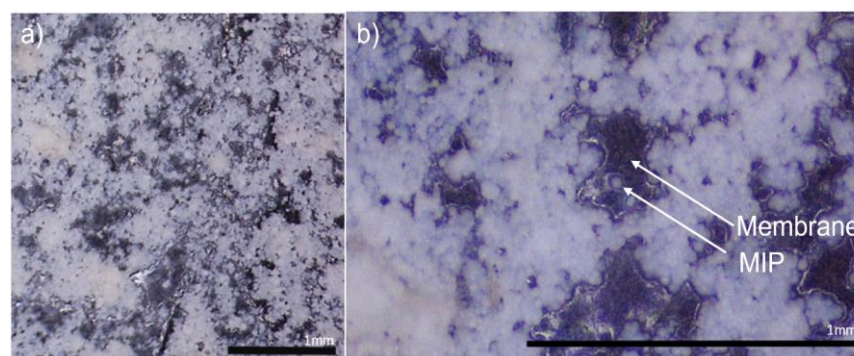

Fig. 3. Pictures of integrated MIPs membrane. The optical microscope with a magnification of 90x was used to study the MIP-membrane surface.

3.2. Initial performances of MIPs

Our previous paper [13] also presents the characteristics of the physicochemical and basic sorption properties of the obtained MIP and NIP materials. Therefore, in the given work, subsequent studies of the sorption properties (e.g. a survey with sorption from the real solutions and selectivity) have been deepened by further analysis. Moreover, the potential use of the obtained microspheres with imprints was proposed to monitor BPA contamination in aqueous solutions using the electro-membrane process, which will be described later in the article. To study the efficiency of removal of BPA from real samples by MIP and NIP, batch mode sorption was performed at room temperature. The results are given in Table 1. The sorption process was performed at ambient temperature because our previous studies with these materials showed that the highest efficiency and differences between the NIP and MIP sorption capacities were observed under these conditions. As can be seen, the MIP microspheres removed about twice as much BPA from tap water as their analogs without molecular imprints.

Table 1
Sorption properties of microspheres from actual samples

Sample	q_{BPA} (mmol/g)	K	log K
MIP	0.19±0.02	1620±20	3.20±0.15
NIP	0.08±0.02	327±15	2.50±0.13

MIP – Molecularly Imprinted Polymer, *NIP* – Non-Imprinted Polymer, q_{BPA} – the amount of BPA adsorbed at equilibrium, was then calculated from Equation (1), *K* – distribution coefficient (equation 3),

The efficiency of removing BPA from tap water with MIP was slightly lower than in the model sample in which the bisphenol A solution was dissolved in deionized water [13]. This value from the model solution was approximately 0.25 mmol/g [13], while from tap water, it is about 0.20 mmol/g. In this case of NIP microspheres, the calculated value of the BPA sorption from the real sample was much smaller than the value obtained during the sorption of BPA from the model solution. The sorption capacity for NIP from tap water was about 0.09 mmol/g, while, in the case of the BPA solution in deionized water, it was about 0.20 mmol/g. However, what is worth highlighting is that in the case of the study with tap water, a more significant difference was observed in the effectiveness of BPA removal between MIP and NIP. This is the most desirable phenomenon, showing that the efficacy of MIPs with a specific imprint is more significant in more complex solutions with other ingredients. Therefore, it can be concluded that these materials will perform well in natural solutions for monitoring BPA in water.

To confirm the imprinting effect and to get a better insight into the behavior of those specific bindings, a study of the sorption on the synthesized materials in the presence of a mixture of BPA and one of the derivatives of phenol was crucial. For this purpose, the competitive binding of the commonly occurring phenol derivative, which can be present in real samples, such as p-nitrophenol, was studied. From the analysis of the data, in the beginning, the distribution coefficients (K_i) were calculated for BPA and NP [35,40]. Moreover, both imprinting and selectivity factors were obtained. The imprinting factor (IF) was calculated as a comparison of the distribution coefficients for binding the same substance by an imprinted and a non-imprinted polymer. Furthermore, taking the ratio of the *IF* parameter for two substances (in this case BPA and NP) and eliminating the partitioning effects between two molecules due to the non-specific impacts, a specific selectivity factor (*S*) was obtained [35, 36]. The results are shown in Table 2.

Table 2
Competitive study

PARAMETER	BPA	NP
K_{MIP} (-)	592±20	254±15
K_{NIP} (-)	378±13	440±16
IF (-)	1.6±0.1	0.6±0.1
S (-)	-	2.7±0.1

BPA – bisphenol A, **NP** – p-nitrophenol, *MIP* – molecularly imprinted polymer, *NIP* – nonimprinted polymer, *K* – distribution coefficient (equation 2), *IF* – imprinting factor (equation 3), *S* – selectivity factor obtained from competitive sorption experiment (equation 4).

The high affinity for BPA for the molecularly imprinted polymer and also at the same time the effectiveness of molecular imprinting was confirmed by the high value of *IF* (1.6 ± 0.1). Furthermore, the selectivity coefficient determined for the MIP sample in relation to NF exceeded the value 1 and was about 2.7 (see Table 2). This proves that the binding of bisphenol A from the mixture studied is preferred. It can be attributed to the presence of specific cavities created by imprinted BPA inducing exactly the effect of molecular imprinting in the polymeric matrix.

3.3. Capacitive deionization process

In recent years, the search for simple and quick methods of monitoring substances present in deficient concentrations in water has become more frequent, which are dangerous even in such low concentrations for the health of people and animals. Because of this, during our work with the obtained MIP and NIP microspheres, it was decided to receive a composite material that could be used in MCDI processes. Creating a method that combines electro-membrane processes and sorption on a material dedicated to a specific substance will allow one to quickly monitor and eliminate the presence of BPA in the aquatic environment. Because of this, in the next step, MIP microspheres were integrated with PVC foils. For this purpose, a suspension of microspheres in THF was dripped directly onto the PVC surfaces. The integrated membranes prepared in this way were then tested for sorption and the possible concentration of BPA in the MCDI process. During the research, the three prominent cases were evaluated: (*i*) the effectiveness of composite materials immediately after receipt, (*ii*) the effectiveness of these films after three months from the moment of receipt, while stored during this time in deionized water, and (*iii*) the effectiveness of BPA removal of these materials from tap water. The modified Ragone plot (mRP) as a CDI parameter was discovered by Kim and Yoon [41] and is a powerful tool for comparing effective sorption. The mRP for fresh foils, foils after three months, and real sample conditions are presented in Fig. 4A. Fresh foils with MIPs reach a remarkably high SAC at ~ 80 mg/g. The same foils after three months reduced this parameter by 25% and got ~ 60 mg/g. The minimal SAC evaluated was determined for the real sample, where the SAC got 40 mg/g, which is 50% less than the fresh material; the decrease in the effectiveness of BPA removal from tap water was also observed during the batch study (see Table 1). With the increase in SAC for fresh foils, the total removal ratio of BPA also increased, which is presented in Fig. 4C. Here, the complete removal of BPA in the adsorption step is almost linear, starting from 10 min. It could be associated with crossing the boundary layers of MIPs and their insertion into the MIPs click system. Bisphenol A is an inert particle without a well-defined charge. Hence, the way of sorption in the 200 μm channel will be predicted according to the diffusion forces, based on the gradient differences between the empty MIP and the circulating BPA solution. The highest sorption rate was investigated for fresh foils, reaching almost 9 mg/g.min. Unfortunately, the sorption rate decreased dramatically after 3 months to 2.2 mg/g.min. According to the mRP, the most effective sorptive material used for the removal of BPA is a freshly prepared membrane with accumulated MIPs. The ratio between ASAR and SAC is optimal and the sorption rate is the highest among investigated configurations. The situation of sorption is closely connected with the energetical parameters. The Wh per gram of MIPs in the foils over time is presented in Fig. 4B. In all the cases evaluated, Wh/g increased over the MCDI operation time. For fresh foils, the system reached about 30 Wh/g; after three months, this value advanced to ~ 60 Wh/g, while for the real sample, it reached 85 Wh/g. This behavior is associated with limited sorption values. The next critical factor is the total removal of BPA. The results are presented in Fig. 4C. Here, the removal of BPA is estimated at 50% for fresh foils and 30% and 23% for foils after 3 months and for real sample investigations, respectively. The removal ratio of BPA is directly proportional correlated to the SAC and ASAR parameters and inversely proportional to the energetical factors. The last section, presented in Fig. 4D, describes the effect of BPA concentration during the desorption steps. Here, different predictions of the concentration of BPA are seen. The back sorption in fresh foils and real samples is caused by the co-ions sorption effect, which is related to the revised sorption during the desorption step on the counter electrode. Finally, a more than 50% concentration of BPA during the desorption step was obtained for fresh foils.

The following parameter of the investigations is the desorption operation. The sorbed BPA in the structure of MIPs was released and concentrated during this stage. The efficiency of desorbed BPA in the convention of sorbed ones is presented in Fig. 5. For all investigated cases, maximum desorption was observed. For fresh foils, the maximum desorption was 82% at 30 min, while for foils after three months, this value shifted to 68% at 10 min. Similar conditions were detected for the real sample, where the maximum desorption reached 58% at 10 min of the desorption step.
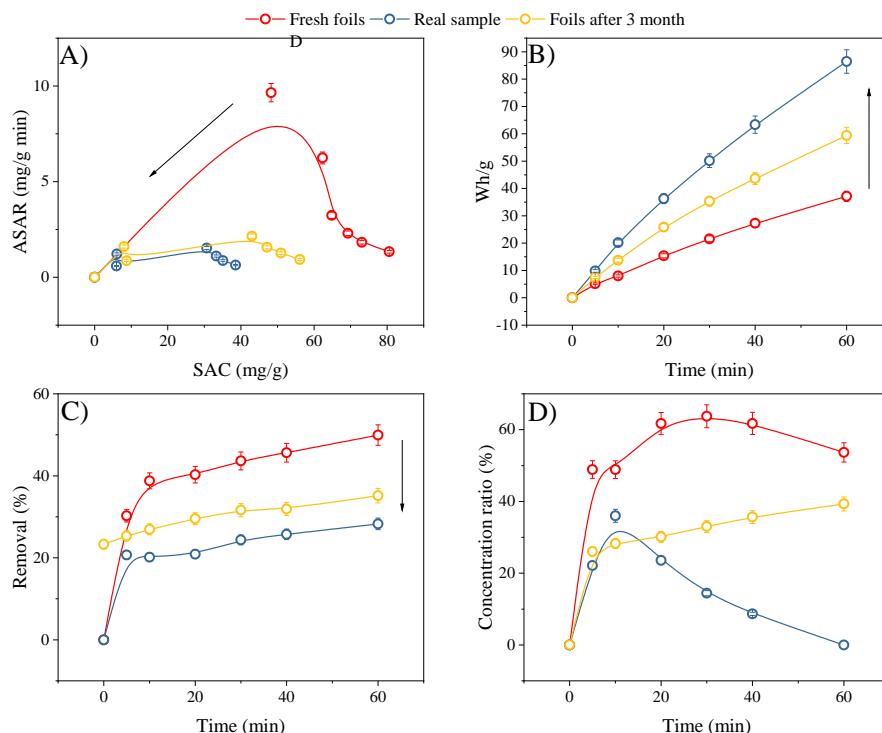
Fig. 4. Modified Ragone plot (A), energetical factors over time (B), removal of BPA (C), and the concentration of BPA during desorption (D). CC mode with a current density of 0.1 A/cm².

One of the most critical questions is why the maximum desorption appears and why the MCDI system does not reach 100% efficiency. The cell of MCDI is composed of symmetrical electrodes covered by the foils wrapped with the same MIPs. Hence, the sorption is predicted at the cathode and anode electrode because BPA does not exhibit any charge; implementing the additional MIP material intensified the SAC. However, during desorption, the polarisation of electrodes is switched, and desorption is begun. The temporarily released particles of BPA were desorbed, but the opposite electrode could interact with these particles and entrap them into the MIPs structure. This behavior is seen in Fig. 5. During the desorption process, the adsorption of co-BPA particles was again adsorbed. This is an explanation for the maximum desorption that occurs.
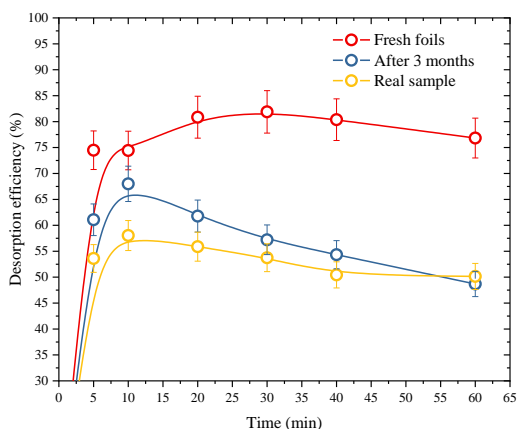

Fig. 5. Desorption efficiency for the evaluated cases. CC mode with current density 0.1 A/cm².

The increasing concentrations of BPA during the MCDI desorption step are presented in Figs. 6A-6C. It could be seen that the highest window of

differences between extracted BPA and concentrated BPA was detected for fresh foils. According to Fig. 6D, the average concentration of BPA reached over 60%. In the cases of antiqued foils and real samples, the concentration reached 10 minutes with values of 38% and 26%, respectively. In addition, the three stages of repeatability were performed to see how stable the membranes were in a short time. Fresh foils in direct three successive processes got more than 60%, while after three months, when the processes were running under the same conditions, these foils reached 14% and 18% for the model solution and the real solution of BPA, respectively.

4. Conclusions

The presented research concerns a new potential use of MIP, which could be successfully applied in the electro-membrane processes. By integrating molecularly imprinted polymers with the polymer film, a material that was used in a modified MCDI process was obtained. This process allowed concentrating solutions of e.g. harmful substances below the detection level in a very short time and, due to this, could serve as an alternative to traditional, long, and often laborious methods used in this case, e.g. the extraction process. The studies showed present the phenomenon of sorption of BPA in the MCDI process with wrapped MIP active materials. The SAC, characteristic of MCDI, reaches a high value of more than 80 mg/g within 60 min. The energetical factor that corresponded to the SAC got an average value of 30 Wh/g for the fresh membranes and decreased to over 80 Wh/g for the older ones. During the desorption process, the re-adsorption of released BPA was noticed. This behavior hurts the desorption efficiency as well as the concentration ratio. Despite this negative phenomenon, the system with composite foils with MIPs could concentrate the BPA with over 60% efficiency. However, the decreased capability of the sorption and desorption processes was noticed after the foils were kept in the water under atmospheric conditions.

Presented research described the possibility of concentration BPA by the MCDI process. To intensify this process, the counter-ion exchange membrane is recommended. This maneuver could help prevent the re-adsorption of released BPA during desorption and increase the concentration ratio to a more satisfactory level.
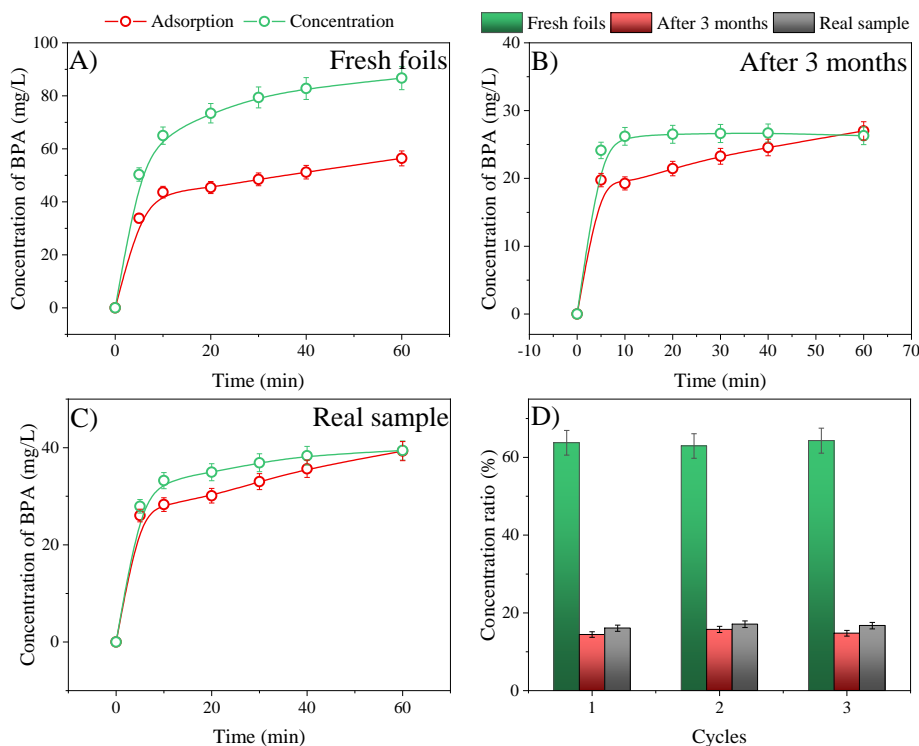
Fig. 6. Concentrated BPA during desorption operation of MCDI for new foils (A), foils after three months (B), and for actual sample (C). Three cycles of repeatability for all cases (t = 20 min, CC mode with current density 0.1 A/cm^2).

Abbreviations

AC	Activated carbon
ASAR	BPA adsorption rate
BPA	Bisphenol A
CDI	Capacitive Deionization
CH	Cyclohexanone
EDA	Ethylenediamine
ENAS	Energy-normalized adsorption of BPA
IF	Imprinting factor
MCDI	Membrane capacitive deionization
MIP	Molecularly imprinted polymer
mRP	Modified Ragone plot
NIP	Non-imprinted polymer
NP	p- nitrophenol
PVC	Poly(vinyl chloride)
SAC	Substance (BPA) adsorption capacity
SEM	Scanning electron microscopy
THF	Tetrahydrofuran

CRedit authorship contribution statement

J. Wolska: Conceptualization, Data curation, Formal analysis, Visualization, Roles/Writing - original draft, Formal analysis, Investigation, Methodology, Writing – review & editing.
A. Siekierka: Formal analysis, Investigation, Methodology, Writing - original draft, Writing – review & editing.
K. Smolińska-Kempisty: Conceptualization, Methodology, Writing - original draft, Visualization, Writing – review & editing.

Funding sources

Declaration of Competing Interest

The authors declare that they have no known competing financial interests or personal relationships that could have appeared to influence the work reported in this paper.

Acknowledgments

References

[1] Global Membrane Technology Market, Market Report, Acmite Market Intelligence / Dechenstr. 17, D-40878 Ratingen, Germany, 2015. www.acmite.com

[2] Membrane Separation Technologies - Global Market Trajectory & Analytics, Report, Global Industry Analysts, Inc, 2022, ID: 1056039, www.researchandmarkets.com

[3] P.Y. Apel, O.V. Bobreshova, A.V. Volkov, V.V. Volkov, V.V. Nikonenko, I.A. Stenina, A.N. Filippov, Y.P. Yampolskii, A.B Yaroslavtsev, Prospects of membrane science development, Membr. Membr. Technol. 1(2) (2019) 45–63. doi: 10.1134/S2517751619020021

[4] S.N. Zulkifli, H.A. Rahim, W.J. Lau, Detection of contaminants in water supply: A review on state-of-the-art monitoring technologies and their applications, Sens. Actuators B Chem. 255(3) (2018) 2657–2689. doi: 10.1016/j.snb.2017.09.078

[5] N. Szczepańska, M. Rutkowska, K. Owczarek, J. Płotka-Wasylka, J. Namieśnik,. Main complications connected with detection, identification, and determination of trace organic constituents in complex matrix samples, TrAC Trends Analyt Chem. 105 (2018) 173–184. doi:10.1016/j.trac.2018.05.005

[6] L. Watt, E. Sisco, Detection of trace drugs of abuse in baby formula using solid-phase microextraction direct analysis in real-time mass spectrometry (SPME-DART-MS), J. Forensic Sci. 66(1) (2021) 172-178. doi:10.1111/1556–4029.14568

[7] Z. Zhang, Trace Level Chemicals Detection By Surface-Enhanced Raman Scattering, ECS Meet. Abstr. MA-2020-01 (33) (2020) 2385. doi: 10.1149/MA2020-01332385mtgabs

[8] Z. Liu, S. Murugesan, S. Ramachandran, P. Jin, Next Generation Oilfield On-site Trace Chemicals Analysis By SERS. Paper presented at the SPE International Conference on Oilfield Chemistry, The Woodlands, Texas, USA, December 2021, Paper Number: SPE-204369-MS. doi:10.2118/204369-MS.

[9] A. Poliwoda, M. Moscipan, P.P. Wieczorek, Application of molecular imprinted polymers for selective solid phase extraction of bisphenol A, Ecol. Chem. Eng. S 23(4) (2016) 651–664. doi:10.1515/eces-2016-0046

[10] S. Piletsky, F. Canfarotta, A. Poma, A.M. Bossi, S. Piletsky, Molecularly imprinted polymers for cell recognition, Trends Biotechnol. 38(4) (2020) 368–387. doi: 10.1016/j.tibtech.2019.10.002

[11] C. Dong, H. Shi, Y. Han, Y. Yang, R. Wang, J. Men, Molecularly imprinted polymers by the surface imprinting technique, Eur. Polym. J. 145 (2021) 110231. doi: 10.1016/j.eurpolymj.2020.110231

[12] J. McClements, L. Bar, P. Singla, F. Canfarotta, A. Thomson, J. Czulak, R.E. Johnson, R.D. Crapnell, C.E. Banks, B. Payne, S. Seyedin, Molecularly Imprinted Polymer Nanoparticles Enable Rapid, Reliable, and Robust Point-of-Care Thermal Detection of SARS-CoV-2, ACS Sens. 7(4) (2022) 1122–1131. doi:10.1021/acssensors.2c00100

[13] J. Wolska, N. Jalilnejad Falizi, Membrane Emulsification Process as a Method for Obtaining Molecularly Imprinted Polymers, Polymers 13(16) (2021) 2830. doi:10.3390/polym13162830

[14] R.A. Hand, E. Piletska, T. Bassindale, G. Morgan, N. Turner, Application of molecularly imprinted polymers in the anti-doping field: sample purification and compound analysis, Analyst 145(14) (2020) 4716–4736. doi: 10.1039/d0an00682c

[15] C. Cáceres, C. Bravo, B. Rivas, E. Moczko, P. Sáez, Y. García, E. Pereira, Molecularly imprinted polymers for the selective extraction of bisphenol a and progesterone from aqueous media, Polymers 10(6) (2018) 679. doi: 10.3390/polym10060679

[16] K. Smolinska-Kempisty, A. Guerreiro, J. Czulak, S. Piletsky, Negative selection of MIPs to create high specificity ligands for glycated hemoglobin, Sens. Actuators B Chem. 301 (2019) 126967. doi: 10.1016/j.snb.2019.126967

[17] W. Li, Q. Zhang, Y. Wang, Y. Ma, Z. Guo, Z. Liu, Controllably prepared aptamer–molecularly imprinted polymer hybrid for high-specificity and high-affinity recognition of target proteins, Anal. Chem. 91(7) (2019) 4831–4837. doi: 10.1021/acs.analchem.9b00465

[18] O.S. Ahmad, T.S. Bedwell, C. Esen, A. Garcia-Cruzand, S.A. Piletsky, Molecularly imprinted polymers in electrochemical and optical sensors, Trends Biotechnol. 37(3) (2019) 294–309. doi: 10.1016/j.tibtech.2018.08.009

[19] Y. Saylan, S. Akgönüllü, H. Yavuz, S. Ünal, A. Denizli, Molecularly imprinted polymer-based sensors for medical applications, Sensors 19(6) (2019) 1279. doi: 10.3390/s19061279

[20] K. Smolinska-Kempisty, J. Czulak, Introduction to nanoMIPS Prepared by Solid-Phase approach as an Alternative for Antibodies in the pseudo-ELISA Diagnostic Assay, Am. J. Biomed. Sci. Res. 5(1) (2019) 5–8. doi: 10.34297/AJBSR.2019.05.000862

[21] K. Smolinska-Kempisty, O.S. Ahmad, A. Guerreiro, K. Karim, E. Piletska, S. Piletsky, New potentiometric sensor based on molecularly imprinted nanoparticles for cocaine detection, Biosens. Bioelectron. 96 (2017) 49–54. doi: 10.1016/j.bios.2017.04.034

[22] Z. Wang, D. Zhang, X. Xiao, C. Su, Z. Li, J. Xue, N. Hu, P. Peng, L. Liao, H. Wang, A highly sensitive and selective sensor for trace uranyl (VI) ion based on a graphene-coated carbon paste electrode modified with ion imprinted polymer, Microchem. J. 155 (2020) 104767. doi: 10.1016/j.microc.2020.104767

[23] R.D. Crapnell, N.C. Dempsey-Hibbert, M. Peeters, A. Tridente, C.E. Banks, Molecularly imprinted polymer based electrochemical biosensors: Overcoming the challenges of detecting vital biomarkers and speeding up diagnosis, Talanta Open 2 (2020) 100018. doi: 10.1016/j.talo.2020.100018

[24] M.A. Beluomini, J.L. da Silva, A.C. de Sá, E. Buffon, T.C. Pereira, N.R. Stradiotto, Electrochemical sensors based on molecularly imprinted polymer on nanostructured carbon materials: A review, J. Electroanal. Chem. 840 (2019) 343–366. doi: 10.1016/j.jelechem.2019.04.005

[25] A. Yusuf, A. Sodiq, A. Giwa, J. Eke, O. Pikuda, G. De Luca, J.L. Di Salvo, S. Chakraborty, A review of emerging trends in membrane science and technology for sustainable water treatment, J. Clean. Prod. 266 (2020), 121867. doi: 10.1016/j.jclepro.2020.121867

[26] N. Kim, J. Lee, S. Kim, S.P. Hong, C. Lee, J. Yoon, C. Kim, Short review of multichannel membrane capacitive deionization: Principle, current status, and future prospect, Appl. Sci. 10(2), (2020) 683. doi: 10.3390/app10020683

[27] A. Siekierka, M. Bryjak, Modified Poly(vinylidene fluoride) by Diethylenetriamine as a Supported Anion Exchange Membrane for Lithium Salt Concentration by Hybrid Capacitive Deionization, Membranes 12(2) (2022) 103. doi: 10.3390/membranes12020103

[28] A. Siekierka, M. Bryjak, Novel anion exchange membrane for concentration of lithium salt in hybrid capacitive deionization, Desalination 452 (2019) 279–289. doi: 10.1016/j.desal.2018.10.009

[29] M.A. Luciano, H. Ribeiro, G.E. Bruch, G.G. Silva, Efficiency of capacitive deionization using carbon materials based electrodes for water desalination, J. Electroanal. Chem. 859 (2020) 113840. doi:10.1016/j.jelechem.2020.113840

[30] Q. Wang, K. Fang, C. He, K. Wang, Ammonia removal from municipal wastewater via membrane capacitive deionization (MCDI) in pilot-scale. Sep. Purif. Technol., 286 (2022) 120469. doi: 10.1016/j.seppur.2022.120469

[31] P. Nie, B. Hu, X. Shang, Z. Xie, M. Huang, J. Liu, Highly efficient water softening by mordenite modified cathode in asymmetric capacitive deionization, Sep. Purif. Technol. 250 (2020) 117240. doi:10.1016/j.seppur.2020.117240

[32] L. Koók, L.F. Rosa, F. Harnisch, J. Žitka, M. Otmar, N. Nemestóthy, P. Bakonyi, J. Kretzschmar, Functional stability of novel homogeneous and heterogeneous cation exchange membranes for abiotic and microbial electrochemical technologies, J. Membr. Sci. 658 (2022) 120705. doi:10.1016/j.memsci.2022.120705

[33] M. Kujawska, T. Zhou, A.W. Trochimczuk, L. Ye, Synthesis of naproxen-imprinted polymer using Pickering emulsion polymerization, J. Mol. Recognit. 31(3) (2018) 2626. doi: 10.1002/jmr.2626

[34] J. Wolska, M. Bryjak, Removal of bisphenol a from aqueous solution by molecularly imprinted polymers, Sep. Sci. Technol. 49(11) (2014) 1643–1653. doi: 10.1080/01496395.2014.906459

[35] J. Wolska, M. Kujawska, P. Cyganowski, Selective sorption of diethyl phthalate on pH-responsive, molecularly imprinted polymeric adsorbents, Sep. Sci. Technol. 55(12) (2020) 2137–2148. doi: 10.1080/01496395.2019.1620778

[36] S.H. Cheong, S. McNiven, A. Rachkov, R. Levi, K. Yano, I. Karube, Testosterone Receptor Binding Mimic Constructed Using Molecular Imprinting, Macromolecules 30 (5) (1997) 1317–1322. doi: 10.1021/ma961014l

[37] A. Siekierka, E. Kmiecik, B. Tomaszewska, K. Wator, M. Bryjak, The evaluation of the effectiveness of lithium separation by hybrid capacitive deionization from geothermal water with the uncertainty measurement application, Desalin. Water Treat. 128 (2018) 259–264. doi: 10.5004/dwt.2018.22870.

[38] A. Siekierka, Preparation of electrodes for hybrid capacitive deionization and its influence on the adsorption behaviour, Sep. Sci. Technol. 55(12) (2020) 2238–2249. doi: 10.1080/01496395.2019.1609032.

[39] A. Siekierka, Lithium and magnesium separation from brines by hybrid capacitive deionization, Desalination 527 (2022) 115569. doi:10.1016/J.DESAL.2022.115569.

[40] D.A. Spivak, Optimization, evaluation, and characterization of molecularly imprinted polymers, Adv. Drug Deliv. Rev. 57(12) (2005) 1779–1794. doi: 10.1016/j.addr.2005.07.012

[41] T. Kim, J. Yoon, CDI Ragone plot as a functional tool to evaluate desalination performance in capacitive deionization, RSC Adv. 5(2) (2015) 1456–1461. doi: 10.1039/C4RA11257A.